Published in final edited form as:
J Mol Endocrinol. 2015 October ; 55(2): 147–158. doi:10.1530/JME-15-0090.

Truncation of POC1A associated with short stature and extreme insulin resistance

Jian-Hua Chen[1,2], **Maria Segni**[3], **Felicity Payne**[4], **Isabel Huang-Doran**[1,2], **Alison Sleigh**[5,6], **Claire Adams**[1,2], **UK10K Consortium**[7], **David B. Savage**[1,2], **Stephen O'Rahilly**[1,2], **Robert K. Semple**[*,1,2], and **Inês Barroso**[*,4,1,2]

[1]The University of Cambridge Metabolic Research Laboratories, Wellcome Trust-MRC Institute of Metabolic Science, Cambridge, UK

[2]The National Institute for Health Research Cambridge Biomedical Research Centre, Cambridge, UK

[3]Dept of Pediatrics, Sapienza University, Rome, Italy

[4]Metabolic Disease Group, Wellcome Trust Sanger Institute, Cambridge, UK

[5]Wolfson Brain Imaging Centre, University of Cambridge, Cambridge, UK

[6]National Institute for Health Research/Wellcome Trust Clinical Research Facility, Cambridge, UK

Abstract

We describe a female proband with primordial dwarfism, skeletal dysplasia, facial dysmorphism, extreme dyslipidaemic insulin resistance and fatty liver associated with a novel homozygous frameshift mutation in *POC1A*, predicted to affect two of the three protein products of the gene. *POC1A* encodes a protein associated with centrioles throughout the cell cycle and implicated in both mitotic spindle and primary ciliary function. Two homozygous mutations affecting all isoforms of *POC1A* have recently been implicated in a similar syndrome of primordial dwarfism, although no detailed metabolic phenotypes were described. Primary cells from the proband we describe exhibited increased centrosome amplification and multipolar spindle formation during mitosis, but showed normal DNA content, arguing against mitotic skipping, cleavage failure or cell fusion. Despite evidence of increased DNA damage in cells with supernumerary centrosomes, no aneuploidy was detected. Extensive centrosome clustering both at mitotic spindles and in primary cilia mitigated the consequences of centrosome amplification, and primary ciliary formation was normal. Although further metabolic studies of patients with *POC1A* mutations are warranted, we suggest that *POC1A* may be added to *ALMS1* and *PCNT* as examples of centrosomal or pericentriolar proteins whose dysfunction leads to extreme dyslipidaemic insulin resistance. Further investigation of links between these molecular defects and adipose tissue

Correspondence: Dr. Robert K. Semple, University of Cambridge Metabolic Research Laboratories, Institute of Metabolic Science, Box 289, Addenbrooke's Hospital, Cambridge CB2 0QQ, UK. Phone: +44 1223 769 035, Fax: +44 1223 330 598, rks16@cam.ac.uk OR Dr. Inês Barroso, The Wellcome Trust Sanger Institute, Wellcome Trust Genome Campus, Cambridge, CB10 1SA, UK. Phone: +44 (0)1223 496 928, Fax: +44 (0)1223 494 919, ib1@sanger.ac.uk.
[*]joint communicating authors
[7]http://www.uk10k.org/consortium.html

Disclosure Statement: The authors have nothing to disclose

Europe PMC Funders Author Manuscripts

dysfunction is likely to yield insights into mechanisms of adipose tissue maintenance and regeneration that are critical to metabolic health.

Keywords

POC1A; Centrosome; Centriole; Primary Cilium; Short stature; Skeletal dysplasia; Insulin resistance; diabetes; dyslipidaemia

Introduction

Insulin action and linear growth are intimately linked, with crosstalk between insulin action and growth hormone/IGF1 signalling at multiple levels in liver and other tissues. This is attested to by the insulin resistance reported in the context of mutations in either the IGF1 receptor (Gannage-Yared, et al. 2013) or the IGF acid labile subunit in humans (Hogler, et al. 2014) and, conversely, by the marked linear growth impairment caused by biallelic INSR mutations (Semple, et al. 2011; Semple, et al. 2010). However growth and insulin action have links beyond these well established endocrine mechanisms. Indeed, a subset of forms of primordial dwarfism caused by cellular defects with no obvious link to insulin action also feature severe dyslipidaemic insulin resistance. These include osteodysplastic primordial dwarfism of Majewski type 2 (MOPDII) (Huang-Doran, et al. 2011), caused by recessive mutations in the pericentrosomal protein PCNT (Rauch, et al. 2008), a recently described form of dwarfism caused by defects in the SUMO ligase NSMCE2 (Payne, et al. 2014a), which is involved in accurate DNA repair in replicating cells, and Bloom syndrome (Diaz, et al. 2006), caused by mutations in the BLM DNA helicase (Ellis, et al. 1995).

Most known forms of primordial dwarfism have not been reported to be associated with insulin resistance, however. Moreover, other pleiotropic disorders have been described affecting either another large component of the centrosome, ALMS1, or another DNA helicase, WRN. Interestingly both of the resulting clinical syndromes, namely Alström syndrome and Werner syndrome, also feature severe insulin resistance and dyslipidaemia (Marshall, et al. 2011; Watanabe, et al. 2013). Increasing understanding of the mechanistic links among insulin action, growth, and cell autonomous defects in centrosomal function and DNA damage repair is likely to yield novel insights into the pathogenesis of systemic insulin resistance, which a substantial body of evidence has implicated as an important mediator of the link between obesity and pathologies such as type 2 diabetes, fatty liver disease, polycystic ovary syndrome and some cancers (Parker, et al. 2011; Savage and Semple 2010; Semple et al. 2011; Stears, et al. 2012).

A new form of primordial dwarfism caused by a homozygous genetic defect in the luminal centriolar protein POC1A was recently described (Koparir, et al. 2015; Sarig, et al. 2012; Shaheen, et al. 2012), and we now add to this by reporting a further affected patient with a frameshift mutation predicted to affect 2 out of 3 POC1A isoforms. This was associated with supernumerary centrosomes and multipolar mitotic spindles in primary cells, and with sustained and extreme dyslipidaemic insulin resistance. This adds a further piece to the puzzle regarding the pathogenic mechanisms linking centrosome/ciliary dysfunction and metabolic disease.

Europe PMC Funders Author Manuscripts

Materials and Methods

Patients and clinical studies

All human studies were approved by the United Kingdom National Health Service Research Ethics Committee. The proband and family provided written informed consent, and studies were conducted in accordance with the principles of the Declaration of Helsinki. For biochemical assays, venous blood was drawn in the fasting state and plasma immediately extracted then stored at −20°C. Insulin, leptin and adiponectin were assayed using two-step, time-resolved AutoDELFIA immunoassays described previously (Semple, et al. 2006). Other analytes were determined in accredited clinical diagnostic laboratories of the referring hospital. For oral glucose tolerance testing, 1.75g glucose/kg was administered after a 10 hour fast and blood samples taken at the times indicated for determination of plasma glucose and insulin.

Body composition was measured by Lunar Prodigy dual-energy X-ray absorptiometry (GE Lunar). Abdominal fat distribution, including hepatic triglyceride content, was assessed by proton magnetic resonance spectroscopy (MRS), using a Siemens 3T Tim Trio MR scanner (Siemens Healthcare, Erlangen, Germany). All protocols have been described in detail previously (Semple et al. 2009).

Genetic Studies

Whole exome sequencing and variant calling of genomic DNA extracted from peripheral blood leukocytes was performed as part of the UK10K Project as described previously (Futema, et al. 2012). Calls were annotated with 1000 Genomes Phase 1 integrated callset v3 allele frequencies (ftp://ftp.1000genomes.ebi.ac.uk/vol1/ftp/phase1/analysis_results/integrated_call_sets) and the NCBI dbSNP database build 137 (ftp://ftp.ncbi.nih.gov/snp/organisms/human_9606/database/b137_archive/organism_data/). Functional annotation was added using Ensembl Variant Effect Predictor v2.8 (McLaren, et al. 2010) against Ensembl build 70. Variants were further annotated with allele frequencies from the Exome Variant Server, NHLBI GO Exome Sequencing Project (ESP), Seattle, WA (URL: http://evs.gs.washington.edu/EVS/) [April 2013], the UK10K Cohorts [REL-2012-06-02] and Exome [REL-2013-04-20] groups (www.UK10K.org) and exome wide sequencing data from 409 control individuals from the CoLaus Cohort (Firmann, et al. 2008). Raw exome sequence data is available from the European Genome-Phenome Archive (https://www.ebi.ac.uk/ega/home; accession numbers EGAN00001083652 and EGAN00001028741).

Variants were defined as potentially functional if they were non-synonymous, resulted in loss or gain of a stop codon or a frameshift, or occurred within essential splice sites. Those unlikely to have a functional impact were removed, as were all heterozygous variants and those found with a non-reference allele frequency greater than 1 % in individuals of European descent from any of the annotated control populations (1000 genomes, UK10K cohorts and exomes, NHLBI exomes and CoLaus exomes). Variants present in the unaffected sister or failing to pass the quality filters were also removed. The remaining

variants were then evaluated as described previously (Payne, et al. 2014b). Comments on predicted alternative protein products of the *POC1A* gene are based on Ensembl build 70.

Cell culture

Dermal fibroblasts derived from skin biopsy of proband and healthy controls were grown in Dulbecco's modified Eagle's medium (DMEM; D6546, Sigma) supplemented with 10% foetal calf serum (HyClone), 4 mM L-glutamine (G7513, Sigma), 1% penicillin-streptomycin (P0781, Sigma) in a humidified incubator (37°C, 5% CO_2). Primary cilia formation was induced by culturing cells in serum-free medium for 24 hours.

cDNA synthesis and sequencing

Total RNA was prepared using RNeasy Mini Kits (Qiagen) with a DNase digestion step to eliminate contaminating DNA, and was quantified on a NanoDrop ND-1000 (Thermo Scientific). First strand cDNA was reverse-transcribed from 400 ng of total RNA using an ImProm-II Reverse Transcription System (Promega) with random hexamer as the primer, according to the manufacturer's protocol. PCR was carried out with a GoTaq Green Master Mix (Promega) and gene-specific primers. Primers were custom-designed and synthesized by Sigma: POC1A forward primer (5′ to 3′) GAACAAGTGATGGTTTGGAAGA, POC1A reverse primer (5′ to 3′) CCCAAGTCCCATGGTACAAA. PCR products were examined by 1% agarose gel followed by Exo1/SAP treatment. Sequencing reactions were performed with a POC1A forward primer (5′ to 3′) CAGAAGTGGACTTCCCTGTC and the above reverse primer.

Western blotting

Cells were washed with ice-cold PBS and harvested in M-PER Mammalian Protein Extraction reagent (Thermo Scientific) containing protease inhibitor mini complete cocktail (Roche) at a 1:7 ratio. Proteins were mixed with an equal volume of Laemmli sample buffer (#161-0737, Bio-Rad), denatured at 95°C and resolved by SDS-PAGE before transfer to polyvinylidene-fluoride membranes using the iBlot system (Invitrogen). Blots were blocked with 5% BSA in TBST (50 mM Tris-HCl, pH7.6, 150 mM NaCl, 0.1% Tween-20) and probed overnight at 4°C with anti-POC1A (HPA040600, Sigma) or anti-calnexin (ab75801, abcam) antibody. Bound primary antibody was detected by horseradish peroxidase conjugated secondary antibodies, followed by Immobilon™ Western chemiluminescent HRP substrate (WBKLS0500, Millipore).

Immunofluorescence analysis

Cells on coverslips were fixed in 4% paraformaldehyde in PBS for 10 min followed by one wash with PBS, permeabilization in 0.2% Triton X-100 in PBS for 5 min, and three washes with PBS (5 min each wash). Coverslips were blocked with blocking buffer (10% horse serum, 1% BSA, 0.02% NaN_3, 1× PBS) for 1 h, washed with PBS and incubated with anti-ALMS1 (ab84892, abcam) and anti-acetylated tubulin (T7451, Sigma-Aldrich) in 1% BSA in PBS overnight at 4°C. After washing with PBS, the cells were incubated with 1:1000 dilution of Alexa Fluor® 488 goat anti-mouse IgG (A11001, Invitrogen) and Alexa Fluor® 555 goat anti-rabbit IgG (A21430, invitrogen) for 45 min at room temperature in the dark,

washed with PBS, mounted on glass slides using the ProLong Gold Antifade Reagent with DAPI (P36931, invitrogen) and inspected with a Zeiss LSM510 Meta confocal laser scanning microscope. For detecting DNA damage, anti-γH2AX antibody (05-636, Millipore) was used according to the above method except that TBS [50 mM Tris-HCl (pH7.4), 150 mM NaCl] instead of PBS was used.

Statistical analysis

Statistical analyses were performed in GraphPad Prism 5.0 (GraphPad Software, San Diego, CA). Statistical significance was determined by pairwise comparisons using a two-tailed unpaired Student's t test with a $p < 0.05$ being considered significant. All data are presented as means SEM.

Results

Case History

The proband is a 26 year-old woman from Italy born at full term to healthy parents who were first cousins. Her birth weight was 2.08kg (−3.1 SDS). The placenta was small and calcified, and surgical repair of a patent ductus arteriosus was performed at 5 months. Linear growth was reported to be retarded throughout development. Menarche occurred precociously at 8.5 years old, and acanthosis nigricans was first noted by the proband's mother at around the same age. At 12.7 years, oral glucose tolerance testing revealed fasting hyperinsulinaemia, with plasma insulin rising to over 5000 pmol/L after a glucose challenge. Fasting glucose and glucose tolerance were normal (Table 1).

Radiological investigation at 11.5 years showed evidence of skeletal dysplasia, with widespread narrowing of the medullary canals of the long bones. The acetabulum appeared dysplastic with a short, thick femoral neck. Middle and distal phalanges were shortened, and bone age was 14.5 years. There was reduced lumbar lordosis, and vertebral bodies had a "dog-like" appearance. There was modestly reduced interpeduncular distance at the base of the lumbar spine, and some lumbosacral transitional vertebrae were present. Chest and skull radiographs were normal.

On examination at 21 years, height was 1.39 m (−4.1 SDS), with relative macrocephaly (head circumference +2 SDS). There were no neurodevelopmental abnormalities. Facial dysmorphism included micrognathia, a prominent nose, posteriorly rotated low set ears, and brachydactyly with widespread flexural acanthosis nigricans extending to the nasolabial crease, perioral and periocular regions. There was moderate facial hirsutism. No nail hypoplasia nor alopecia was found (Figure 1). Body mass index was 24.5 kg/m^2, with a mildly centripetal pattern of adiposity. Oral glucose tolerance testing revealed sustained fasting and post-prandial severe hyperinsulinaemia, again with normal fasting glucose and impaired glucose tolerance (Table 1). There was severe hypertriglyceridaemia and a low HDL cholesterol, plasma leptin was elevated and adiponectin severely suppressed, and total testosterone was elevated despite a low serum SHBG. Despite these severe biochemical features of insulin resistance, most commonly seen in the face of morbid obesity, the total body fat content, assessed using dual energy X-ray absorptiometry, was normal.

Nevertheless magnetic resonance spectroscopy revealed grossly elevated hepatic triglyceride content relative to water (Table 2). Metformin was commenced and titrated to 1.5 g per day in divided doses.

At 26 years old oral glucose tolerance testing confirmed persisting extreme insulin resistance (Table 1), still with normal glucose tolerance, while treated with 1.5 g per day of metformin. Severe dyslipidaemia also persisted, with serum triglycerides of 25.0 mmol/l, and HDL cholesterol 0.57 mmol/l. Mildly elevated serum ALT, AST and γGT were consistent once again with significant fatty liver.

The proband's unaffected younger sister had a height of 1.63cm at 18 years (−0.09 SDS). Both parents were of normal stature. There was no evidence of short stature nor severe insulin resistance within the extended family, however the proband's father and both grandmothers, of lean build, were reportedly diagnosed with type 2 diabetes mellitus in their sixth decade. The proband's father had a normal HbA1c on therapy with metformin only, while oral glucose tolerance testing in the proband's mother and sister revealed normal levels of both glucose and insulin at baseline and after 120 minutes.

Genetic Analysis

Given parental consanguinity it was hypothesised that the syndrome was caused by a homozygous loss-of-function mutation not shared by the proband's unaffected sister. To address this, exome-wide sequencing of the proband and her sister was performed. The resulting list of homozygous variants was filtered to exclude those unlikely to alter protein function, also homozygous in the sister, or common in control populations. Seven such variants were thus identified and validated by Sanger sequencing (Supplementary Table 1), among which was a novel single nucleotide deletion (c.1048delC) in *POC1A* (NM_001161580) that was absent from all control populations and was predicted to cause a frameshift and premature truncation of the protein product (p.Q250Rfs*4) (Figure 2A). Both parents and sister were heterozygous for this deletion.

POC1A is a centrosomal protein that localises to both the inner luminal walls and proximal ends of centrioles (Brito, et al. 2012) and plays a role in centriole formation and maintenance (Venoux, et al. 2013). It harbours seven N terminal WD40 domains in series, commonly involved in the assembly of multi-protein complexes, followed by a spacer region and C terminal coiled coil domain that is removed by the frameshift mutation we identified (Figure 2A).

Although we hypothesised a recessive disorder given parental consanguinity, as an additional screen for alternative causes of insulin resistance we also examined variants in other genes previously shown to produce severe insulin resistance (*INSR*,*PIK3R1*,*AKT2*,*TBC1D4*,*LMNA*,*PPARG*,*BSCL2*, *AGPAT2*,*PTRF*,*CAV1*,*PCNT*,*NSMCE2*,*ALMS1*,*WRN, and BLM*). After removing any variants found in the listed genes with a non-reference allele frequency greater than 1 % in any of the control populations, or unlikely to have a functional impact (determined as above), only 2 variants remained (ALMS1 p.Ile3144Val and AGPAT2 p.Arg159Cys). Both of these heterozygous variants were also seen in at least two of the control populations

(albeit with a non-reference allele frequency below 1%) and are extremely unlikely to be causal on their own given the very well established recessive mode of inheritance for both the associated disorders. As three recent studies associated different homozygous mutations in *POC1A* with primordial dwarfism and facial dysmorphism highly similar to that of the proband in this case (Sarig et al. 2012; Shaheen et al. 2012), this rare frameshift variant was deemed to be the cause of the syndrome we describe.

Primary cell studies

Primary dermal fibroblast cultures were established from the proband and grew well. No deficit in insulin-stimulated AKT phosphorylation was observed, consistent with a lack of any defect in proximal insulin signalling (Supplementary Figure 1). However western blotting failed to detect expression of either full length wild-type or truncated POC1A (Figure 2B). Two shorter isoforms of POC1A have been predicted, one lacking the N-terminal 38 amino acids due to alternative start codon usage, and the other lacking 48 amino acids due to alternative splicing of exon 10. Exon 10 encodes a large part of the spacer region and a small part of the coiled coil domain of the longest isoform of POC1A (407 amino acids long) (Figure 2C), and is the site of the mutation identified in this study. PCR amplification of cDNA using primers flanking exon 10 produced two products of the sizes expected for exon 10+ and exon 10− transcripts (Figure 2D), suggesting that a wild type exon 10− isoform may still be produced. Indeed, in two healthy control cell lines the predominant PCR product was from the exon 10+ isoform whereas in the patient cells the predominant PCR product was from the exon 10− isoform (Figure 2D). The antibody used in immunoblotting studies was raised against a region of which a third is encoded by exon 10, and so it is plausible that this putative shorter protein is indeed expressed, but not detected in the proband's cells.

As mutations in *POC1A* have been associated with centrosome amplification (Koparir et al. 2015; Sarig et al. 2012; Shaheen et al. 2012), we next examined centrosome number in the proband's fibroblasts using immunostaining with antibody against ALMS1, a protein localized to the proximal ends of centrioles (Knorz, et al. 2010). About 12% of interphase cells showed centrosomal amplification with centrosome number ranging from 3 to 10 per cell. During the mitotic phase, around 39% of cells showed multipolar spindle formation (Figure 3A and supplementary Figure 2). In both cases, proband cells showed over ten-fold increase in the frequency of centrosomal amplification and multipolar spindle formation compared to the control cells.

Despite evidence of centrosome amplification, the proliferation rate of the proband's cells, measured by BrdU incorporation, did not show any difference compared to the control cells (Supplementary Figure 3). Although centrosome amplification can lead to multipolar spindle formation, we found that primary cilia in proband dermal fibroblasts were of normal length and frequency (Supplementary Figure 4), with multiple centrosomes always clustered at the basal body of a single cilium (Figure 3B).

Supernumerary centrioles/centrosomes may arise due to overduplication, aberrant *de novo* synthesis, mitotic skipping, cleavage failure or cell fusion (Anderhub, et al. 2012). DNA content analysis by FACS revealed a cell cycle distribution profile for the proband's dermal

fibroblasts that was indistinguishable from healthy control cells (Supplementary Figure 5A), suggesting that centrosome amplification in the proband's cells was due to overduplication rather than cleavage failure, mitotic skipping or cell fusion, as these would produce cells with 8N DNA content. In line with this, karyotype analysis in the proband fibroblasts was normal (Supplementary Figure 5B).

As for primary cilia, where centrosome clustering was seen in the region of the basal body (Figure 3B), clusters of centrosomes were also seen at many mitotic spindles (Figure 4A). Centrosome clustering prevents multipolar cell division, however it can lead to syntelic or merotelic kinetochore attachments which can lead in turn to chromosome mis-segregation (Anderhub et al. 2012; Vitre and Cleveland 2012). One consequence of chromosome mis-segregation, if not corrected by the activity of Aurora-B, is the formation of anaphase bridges or lagging chromosomes, detectable as micronuclei (Anderhub et al. 2012; Vitre and Cleveland 2012). These abnormalities were observed at a higher level in the proband cells with centrosome amplification (Figure 4B) with micronuclei staining avidly for anti-γH2AX, suggesting the presence of double stranded DNA breaks (Figure 4C). This was consistent with Western blotting which showed γH2AX to be higher in proband cells than in those from two healthy control individuals (Supplementary Figure 6).

Discussion

We used exome-wide sequencing to investigate a single proband with consanguineous parents and a rare syndrome of primordial dwarfism, facial dysmorphism, skeletal dysplasia, and extreme, dyslipidaemic insulin resistance. We identified 7 rare, functional homozygous variants, among which was a frameshift mutation in *POC1A*, which was associated during the course of our study by three groups with a similar syndrome in five consanguineous families from the Middle East (Koparir et al. 2015; Sarig et al. 2012; Shaheen et al. 2012). Three of these families harboured one of two missense mutations (Koparir et al. 2015; Sarig et al. 2012), while the other three families had in common an early nonsense mutation, although cellular studies suggested significant translational readthrough of the mutation (Shaheen et al. 2012).

On the basis of the close similarity among the reported phenotypes it is highly likely that the new *POC1A* variant is the cause of the syndrome we describe. The growth parameters, facial dysmorphism and skeletal features of the proband in this report are highly similar to other published cases (Koparir et al. 2015), and although the large majority of patients reported to date are of prepubertal age, one other patient has been described with precocious puberty (Koparir et al. 2015), which may play a role in the short final height of the proband we describe. There are significant phenotypic differences among patients reported to date, however, Most prominently, the proband we describe had no ectodermal dysplasia, reported in three of four families to date (Koparir et al. 2015; Shaheen et al. 2012), and, conversely, did have extreme, dyslipidaemic insulin resistance, which was not clearly described in other reports. Differing genetic backgrounds may contribute to these differences, as suggested by the occurrence of type 2 diabetes of onset in middle age in several members of the family we describe, albeit without the extreme insulin resistance of the proband. We could not attribute this to rare variants in other genes previously associated with Mendelian insulin resistance,

and nor were there any obvious functional interactions between POC1A and other genes harbouring rare homozygous variants in this study. Nevertheless such interactions cannot be formally excluded in an individual patient, and nor can an effect of heterozygous POC1A loss of function on susceptibility to type 2 diabetes be ruled out based on the data we present.

Some of the phenotypic differences may alternatively be explained by the differing nature of the *POC1A* mutations involved in each report: previous cases were attributed to *POC1A* hypomorphism due to partial readthrough of a premature nonsense mutation in one report (Shaheen et al. 2012), and to rare missense mutations in two others (Koparir et al. 2015; Sarig et al. 2012). In all cases all protein products of the gene were predicted to be affected. In the current report, in contrast, we identified a frameshift mutation predicted to abolish expression of two out of three protein isofoms. We provide evidence that one of the predicted *POC1A* mRNA species, lacking exon 10 and thus the frameshift mutation, is indeed expressed, although formal proof of the existence of the corresponding exon 10− isoform of POC1A protein is lacking. The exon 10− isoform retains the WD40 domain, required for targeting POC1A to centrioles but lacks almost half of the coiled coil POC1 domain, implicated in interactions with other proteins (Keller, et al. 2009). It is therefore conceivable that wild type exon 10− POC1A protein, if expressed, can partially compensate for the loss of the exon 10+ isoforms in our patient. Examination of further cases will be required to build a more robust view of genotype-phenotype correlation.

Despite the lack of detailed metabolic assessment reported for other cases, 2 affected males in one report were said to have developed unusually early type 2 diabetes (Shalev, et al. 2012), at 20 and 24 years old, a common feature of severe insulin resistance. Moreover a further patient has been identified with clearly demonstrated severely dyslipidaemic insulin resistance (Prof. Fowzan Alkuraya, King Faisal Specialist Hospital and Research Center, Riyadh, personal communication), strongly suggesting that severe insulin resistance is a significant component of the syndrome associated with genetic defects in *POC1A*. It is notable that the majority of patients described to date are of prepubertal age (Koparir et al. 2015), when even many highly penetrant forms of Mendelian severe insulin resistance are yet to be clinically expressed, and we suggest that metabolic evaluation for severe insulin resistance is warranted for patients with this syndrome from puberty onwards.

The insulin resistance subphenotype we report, including severe dyslipidaemia, suppressed adiponectin and severe fatty liver is closely similar to that shared by lipodystrophy (Semple et al. 2011) and severe obesity, and also, interestingly, by both Alström syndrome (Collin, et al. 2002; Hearn, et al. 2002) and MOPDII (Rauch et al. 2008; Willems, et al. 2010), each accounted for by defects in large centriolar or pericentriolar proteins. Alström syndrome is widely regarded as a ciliopathy (Girard and Petrovsky 2011), while in MOPDII the core cellular defect appears to be inefficient mitosis (Klingseisen and Jackson 2011; Rauch 2011). A wide number of other primary ciliopathies, notably the Bardet Biedl syndrome group, are known, but it is not clear that they feature insulin resistance that is out of proportion to the degree of obesity, while most forms of primordial dwarfism have also not been associated with severe insulin resistance. It thus appears that only a subset of genetic defects affecting the centrosome give rise to extreme, dyslipidaemic insulin resistance.

Further investigation of the pathogenesis of these unusual metabolic phenocopies of the prevalent metabolic syndrome is likely to yield novel information relevant to common disease as well as to these rare Mendelian disorders.

The primary cell phenotype we describe is in key respects consistent with previous studies, including centrosomal amplification and multipolar spindle formation, which we suggest is accounted for by primary centrosome over-duplication. The three fold greater level of cells with supernumerary centrosomes seen during mitotis than during interphase is likely to be a consequence of prolonged mitosis due to kinetochore mis-attachment and chromosome mis-segregation (Silkworth, et al. 2009). Although the mechanisms by which cells keep centrosome numbers constant during cell division remain to be fully elucidated it is generally believed that two distinct “rules” apply. The first stipulates that centrosomes duplicate once only per cell cycle and the second that only one daughter centriole is produced per parent centriole (Nigg 2007). Although many centrosomal proteins have been identified, major centriole duplication factors are limited, with SAS6 and Plk4 being the best characterised (Holland, et al. 2010; Kleylein-Sohn, et al. 2007; Strnad, et al. 2007). Overexpression of SAS6 and Plk4 causes near-simultaneous formation of multiple daughter centrioles (Kleylein-Sohn et al. 2007; Strnad et al. 2007), and Plk4 kinase activity normally limits centrosome overduplication by autoregulating its own stability (Holland, et al. 2012; Holland et al. 2010). Investigating whether POC1A interacts functionally with these factors is an obvious route for further study.

Although we confirm multipolar spindle formation, multi-cilia formation was not observed. This is consistent with previous knockdown studies which showed that the paralogue *POC1B*, but not *POC1A*, is required for ciliogenesis in human cells (Pearson, et al. 2009). Similarly, Venoux et al recently observed that although *POC1A* and *POC1B* act together in human cells to ensure centriole integrity, only *POC1B* had additional, non-redundant functions in cell proliferation (Venoux et al. 2013). On the other hand ciliary formation was reported to be severely suppressed in primary skin cells from one previous patient studied, although sonic hedgehog (SHH) signalling in *POC1A*-knockdown cells was unaffected (Shaheen et al. 2012). Whether this discrepancy has a methodological basis, or whether it relates to the different molecular defects present in *POC1* in these different studies, remains unclear.

Multiple centrosomes were always clustered at the basal body of a single cilium in our patient cells. Such centrosome clustering is believed to be a survival mechanism, permitting cells to avoid multipolar division (Ganem, et al. 2009; Vitre and Cleveland 2012) by undergoing pseudo-bipolar mitosis (Anderhub et al. 2012; Vitre and Cleveland 2012). Chromosome mis-segregation can also lead to aneuploidy and although karyotypic analysis failed to detect this in the proband cells, it remains possible that low levels of aneuploidy in vivo resulting from chromosome mis-segregation could play some role in causing cellular malfunction in our patient, for example via proteotoxic and energetic stress which can cause cell cycle arrest or apoptosis (Pfau and Amon 2012).

In summary, we describe a novel frameshift mutation in *POC1A* in association with short stature, skeletal dysplasia and extreme, dyslipidaemic insulin resistance. The truncating

Europe PMC Funders Author Manuscripts

mutation abolished expression of the mutation-bearing exon10+ isoform in patient, although the wild type exon 10− isoform may still be expressed and thereby partially compensate for abolished expression of exon 10+ isoforms. Primary dermal fibroblasts exhibited centrosome amplification with evidence of increased DNA damage, but no readily detectable aneuploidy.

Supplementary Material

Refer to Web version on PubMed Central for supplementary material.

Acknowledgements

This work was supported by the Wellcome Trust [grant numbers WT098498, WT098051,WT095515, and WT091310]; the Medical Research Council [MRC_MC_UU_12012/5]; the United Kingdom National Institute for Health Research (NIHR) Cambridge Biomedical Research Centre. We are grateful for access to exome sequence data from the CoLaus cohort, which was sequenced as part of a partnership between the Wellcome Trust Sanger Institute, the CoLaus principal investigators and the Quantitative Sciences department of GlaxoSmithKline. We also thank the NHLBI GO Exome Sequencing Project and its ongoing studies which provided exome variant calls for comparison, namely the Lung GO (HL-102923), the WHI (HL-102924), the Broad GO (HL-102925), the Seattle GO (HL-102926) and the Heart GO (HL-103010) Sequencing Projects. A full list of the investigators contributing to the UK10K Consortium is available from www.UK10K.org.

References

Anderhub SJ, Kramer A, Maier B. Centrosome amplification in tumorigenesis. Cancer Lett. 2012; 322:8–17. [PubMed: 22342684]

Brito DA, Gouveia SM, Bettencourt-Dias M. Deconstructing the centriole: structure and number control. Curr Opin Cell Biol. 2012; 24:4–13. [PubMed: 22321829]

Collin GB, Marshall JD, Ikeda A, So WV, Russell-Eggitt I, Maffei P, Beck S, Boerkoel CF, Sicolo N, Martin M, et al. Mutations in ALMS1 cause obesity, type 2 diabetes and neurosensory degeneration in Alstrom syndrome. Nat Genet. 2002; 31:74–78. [PubMed: 11941369]

Diaz A, Vogiatzi MG, Sanz MM, German J. Evaluation of short stature, carbohydrate metabolism and other endocrinopathies in Bloom's syndrome. Horm Res. 2006; 66:111–117. [PubMed: 16763388]

Ellis NA, Groden J, Ye TZ, Straughen J, Lennon DJ, Ciocci S, Proytcheva M, German J. The Bloom's syndrome gene product is homologous to RecQ helicases. Cell. 1995; 83:655–666. [PubMed: 7585968]

Firmann M, Mayor V, Vidal PM, Bochud M, Pecoud A, Hayoz D, Paccaud F, Preisig M, Song KS, Yuan X, et al. The CoLaus study: a population-based study to investigate the epidemiology and genetic determinants of cardiovascular risk factors and metabolic syndrome. BMC Cardiovasc Disord. 2008; 8:6. [PubMed: 18366642]

Futema M, Plagnol V, Whittall RA, Neil HA, Humphries SE. Use of targeted exome sequencing as a diagnostic tool for Familial Hypercholesterolaemia. J Med Genet. 2012; 49:644–649. [PubMed: 23054246]

Ganem NJ, Godinho SA, Pellman D. A mechanism linking extra centrosomes to chromosomal instability. Nature. 2009; 460:278–282. [PubMed: 19506557]

Gannage-Yared MH, Klammt J, Chouery E, Corbani S, Megarbane H, Abou Ghoch J, Choucair N, Pfaffle R, Megarbane A. Homozygous mutation of the IGF1 receptor gene in a patient with severe pre- and postnatal growth failure and congenital malformations. Eur J Endocrinol. 2013; 168:K1–7. [PubMed: 23045302]

Girard D, Petrovsky N. Alstrom syndrome: insights into the pathogenesis of metabolic disorders. Nat Rev Endocrinol. 2011; 7:77–88. [PubMed: 21135875]

Hearn T, Renforth GL, Spalluto C, Hanley NA, Piper K, Brickwood S, White C, Connolly V, Taylor JF, Russell-Eggitt I, et al. Mutation of ALMS1, a large gene with a tandem repeat encoding 47 amino acids, causes Alstrom syndrome. Nat Genet. 2002; 31:79–83. [PubMed: 11941370]

Hogler W, Martin DD, Crabtree N, Nightingale P, Tomlinson J, Metherell L, Rosenfeld R, Hwa V, Rose S, Walker J, et al. IGFALS gene dosage effects on serum IGF-I and glucose metabolism, body composition, bone growth in length and width, and the pharmacokinetics of recombinant human IGF-I administration. J Clin Endocrinol Metab. 2014; 99:E703–712. [PubMed: 24423360]

Holland AJ, Fachinetti D, Zhu Q, Bauer M, Verma IM, Nigg EA, Cleveland DW. The autoregulated instability of Polo-like kinase 4 limits centrosome duplication to once per cell cycle. Genes Dev. 2012; 26:2684–2689. [PubMed: 23249732]

Holland AJ, Lan W, Niessen S, Hoover H, Cleveland DW. Polo-like kinase 4 kinase activity limits centrosome overduplication by autoregulating its own stability. J Cell Biol. 2010; 188:191–198. [PubMed: 20100909]

Huang-Doran I, Bicknell LS, Finucane FM, Rocha N, Porter KM, Tung YC, Szekeres F, Krook A, Nolan JJ, O'Driscoll M, et al. Genetic defects in human pericentrin are associated with severe insulin resistance and diabetes. Diabetes. 2011; 60:925–935. [PubMed: 21270239]

Keller LC, Geimer S, Romijn E, Yates J 3rd, Zamora I, Marshall WF. Molecular architecture of the centriole proteome: the conserved WD40 domain protein POC1 is required for centriole duplication and length control. Mol Biol Cell. 2009; 20:1150–1166. [PubMed: 19109428]

Kleylein-Sohn J, Westendorf J, Le Clech M, Habedanck R, Stierhof YD, Nigg EA. Plk4-induced centriole biogenesis in human cells. Dev Cell. 2007; 13:190–202. [PubMed: 17681131]

Klingseisen A, Jackson AP. Mechanisms and pathways of growth failure in primordial dwarfism. Genes Dev. 2011; 25:2011–2024. [PubMed: 21979914]

Knorz VJ, Spalluto C, Lessard M, Purvis TL, Adigun FF, Collin GB, Hanley NA, Wilson DI, Hearn T. Centriolar association of ALMS1 and likely centrosomal functions of the ALMS motif-containing proteins C10orf90 and KIAA1731. Mol Biol Cell. 2010; 21:3617–3629. [PubMed: 20844083]

Koparir A, Karatas OF, Yuceturk B, Yuksel B, Bayrak AO, Gerdan OF, Sagiroglu MS, Gezdirici A, Kirimtay K, Selcuk E, et al. Novel POC1A mutation in primordial dwarfism reveals new insights for centriole biogenesis. Hum Mol Genet. 2015

Marshall JD, Beck S, Maffei P, Naggert JK. Alstrom syndrome. Eur J Hum Genet. 2007; 15:1193–1202. [PubMed: 17940554]

Marshall JD, Maffei P, Collin GB, Naggert JK. Alstrom syndrome: genetics and clinical overview. Curr Genomics. 2011; 12:225–235. [PubMed: 22043170]

McLaren W, Pritchard B, Rios D, Chen Y, Flicek P, Cunningham F. Deriving the consequences of genomic variants with the Ensembl API and SNP Effect Predictor. Bioinformatics. 2010; 26:2069–2070. [PubMed: 20562413]

Mihai CM, Catrinoiu D, Marshall J, Stoicescu R, Tofolean IT. Cilia, Alstrom syndrome-- molecular mechanisms and therapeutic perspectives. J Med Life. 2008; 1:254–261. [PubMed: 20108502]

Minton JA, Owen KR, Ricketts CJ, Crabtree N, Shaikh G, Ehtisham S, Porter JR, Carey C, Hodge D, Paisey R, et al. Syndromic obesity and diabetes: changes in body composition with age and mutation analysis of ALMS1 in 12 United Kingdom kindreds with Alstrom syndrome. J Clin Endocrinol Metab. 2006; 91:3110–3116. [PubMed: 16720663]

Nigg EA. Centrosome duplication: of rules and licenses. Trends Cell Biol. 2007; 17:215–221. [PubMed: 17383880]

Parker VE, Savage DB, O'Rahilly S, Semple RK. Mechanistic insights into insulin resistance in the genetic era. Diabet Med. 2011; 28:1476–1486. [PubMed: 21992440]

Payne F, Colnaghi R, Rocha N, Seth A, Harris J, Carpenter G, Bottomley WE, Wheeler E, Wong S, Saudek V, et al. Hypomorphism in human NSMCE2 linked to primordial dwarfism and insulin resistance. J Clin Invest. 2014a; 124:4028–4038. [PubMed: 25105364]

Payne F, Lim K, Girousse A, Brown RJ, Kory N, Robbins A, Xue Y, Sleigh A, Cochran E, Adams C, et al. Mutations disrupting the Kennedy phosphatidylcholine pathway in humans with congenital lipodystrophy and fatty liver disease. Proc Natl Acad Sci U S A. 2014b; 111:8901–8906. [PubMed: 24889630]

Pearson CG, Osborn DP, Giddings TH Jr. Beales PL, Winey M. Basal body stability and ciliogenesis requires the conserved component Poc1. J Cell Biol. 2009; 187:905–920. [PubMed: 20008567]

Pfau SJ, Amon A. Chromosomal instability and aneuploidy in cancer: from yeast to man. EMBO Rep. 2012; 13:515–527. [PubMed: 22614003]

Rauch A. The shortest of the short: pericentrin mutations and beyond. Best Pract Res Clin Endocrinol Metab. 2011; 25:125–130. [PubMed: 21396579]

Rauch A, Thiel CT, Schindler D, Wick U, Crow YJ, Ekici AB, van Essen AJ, Goecke TO, Al-Gazali L, Chrzanowska KH, et al. Mutations in the pericentrin (PCNT) gene cause primordial dwarfism. Science. 2008; 319:816–819. [PubMed: 18174396]

Sarig O, Nahum S, Rapaport D, Ishida-Yamamoto A, Fuchs-Telem D, Qiaoli L, Cohen-Katsenelson K, Spiegel R, Nousbeck J, Israeli S, et al. Short stature, onychodysplasia, facial dysmorphism, and hypotrichosis syndrome is caused by a POC1A mutation. Am J Hum Genet. 2012; 91:337–342. [PubMed: 22840363]

Savage DB, Semple RK. Recent insights into fatty liver, metabolic dyslipidaemia and their links to insulin resistance. Curr Opin Lipidol. 2010; 21:329–336. [PubMed: 20581678]

Semple RK, Savage DB, Cochran EK, Gorden P, O'Rahilly S. Genetic syndromes of severe insulin resistance. Endocr Rev. 2011; 32:498–514. [PubMed: 21536711]

Semple , RK.; Savage , DB.; Halsall , DJ.; O'Rahilly , S. Syndromes of Severe Insulin Resistance and/or Lipodystrophy. In: Weiss , RE.; Refetoff , S., editors. Genetic Diagnosis of Endocrine Disorders. Elsevier; 2010. p. 39

Semple RK, Sleigh A, Murgatroyd PR, Adams CA, Bluck L, Jackson S, Vottero A, Kanabar D, Charlton-Menys V, Durrington P, et al. Postreceptor insulin resistance contributes to human dyslipidemia and hepatic steatosis. J Clin Invest. 2009; 119:315–322. [PubMed: 19164855]

Semple RK, Soos MA, Luan J, Mitchell CS, Wilson JC, Gurnell M, Cochran EK, Gorden P, Chatterjee VK, Wareham NJ, et al. Elevated plasma adiponectin in humans with genetically defective insulin receptors. J Clin Endocrinol Metab. 2006; 91:3219–3223. [PubMed: 16705075]

Shaheen R, Faqeih E, Shamseldin HE, Noche RR, Sunker A, Alshammari MJ, Al-Sheddi T, Adly N, Al-Dosari MS, Megason SG, et al. POC1A truncation mutation causes a ciliopathy in humans characterized by primordial dwarfism. Am J Hum Genet. 2012; 91:330–336. [PubMed: 22840364]

Shalev SA, Spiegel R, Borochowitz ZU. A distinctive autosomal recessive syndrome of severe disproportionate short stature with short long bones, brachydactyly, and hypotrichosis in two consanguineous Arab families. Eur J Med Genet. 2012; 55:256–264. [PubMed: 22440536]

Silkworth WT, Nardi IK, Scholl LM, Cimini D. Multipolar spindle pole coalescence is a major source of kinetochore mis-attachment and chromosome mis-segregation in cancer cells. PLoS One. 2009; 4:e6564. [PubMed: 19668340]

Stears A, O'Rahilly S, Semple RK, Savage DB. Metabolic insights from extreme human insulin resistance phenotypes. Best Pract Res Clin Endocrinol Metab. 2012; 26:145–157. [PubMed: 22498245]

Strnad P, Leidel S, Vinogradova T, Euteneuer U, Khodjakov A, Gonczy P. Regulated HsSAS-6 levels ensure formation of a single procentriole per centriole during the centrosome duplication cycle. Dev Cell. 2007; 13:203–213. [PubMed: 17681132]

Venoux M, Tait X, Hames RS, Straatman KR, Woodland HR, Fry AM. Poc1A and Poc1B act together in human cells to ensure centriole integrity. J Cell Sci. 2013; 126:163–175. [PubMed: 23015594]

Vitre BD, Cleveland DW. Centrosomes, chromosome instability (CIN) and aneuploidy. Curr Opin Cell Biol. 2012; 24:809–815. [PubMed: 23127609]

Watanabe K, Kobayashi K, Takemoto M, Ishibashi R, Yamaga M, Kawamura H, Fujimoto M, Ishikawa T, Onishi S, Okabe E, et al. Sitagliptin improves postprandial hyperglycemia by inhibiting glucagon secretion in Werner syndrome with diabetes. Diabetes Care. 2013; 36:e119. [PubMed: 23881973]

Willems M, Genevieve D, Borck G, Baumann C, Baujat G, Bieth E, Edery P, Farra C, Gerard M, Heron D, et al. Molecular analysis of pericentrin gene (PCNT) in a series of 24 Seckel/microcephalic osteodysplastic primordial dwarfism type II (MOPD II) families. J Med Genet. 2010; 47:797–802. [PubMed: 19643772]

Figure 1. Clinical appearance of proband

(A and B) Facial appearance of the proband showing facial dysmorphism including a triangular face with a prominent nose, posteriorly rotated low set ears, acanthosis nigricans extending to the nasolabial crease, perioral and periocular regions, and facial hirsutism. No alopecia was found. Written informed consent was given by the proband for use of clinical images.

Europe PMC Funders Author Manuscripts

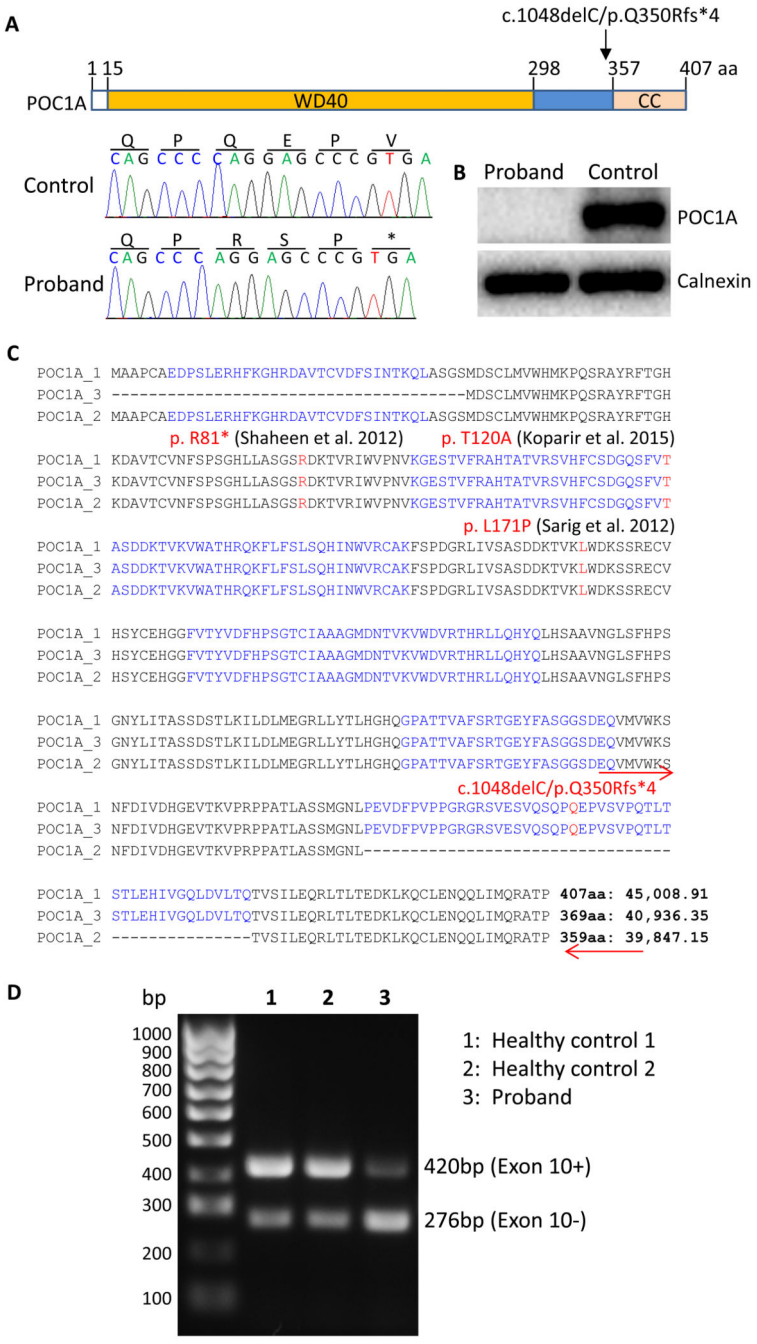

Figure 2. POC1A frameshift mutation and detection of its protein and mRNA expression

(A) Schematic of POC1A showing that the protein contains a WD40-repeat domain and a coiled coil (CC) domain separated by a spacer region. The mutation site is indicated by the arrow and the deletion mutation and resulting frameshift are shown in a sequence chromatogram. (B) Western blot analysis of primary dermal fibroblast lysates of the proband and of a healthy control. (C) Three splicing variants of POC1A were aligned and mutation in the proband in this study as well as mutations described in three previous reports were indicated in red letters. Amino acids encoded by 11 exons were indicated in black and blue

letters. Numbers of amino acids and the predicted molecular sizes of each isoforms were indicated at the end of each isoform sequence. Locations of primers used for PCR to reveal the expected alternative splicing of exon 10 were indicated by red arrows (the reverse primer was in the 3′ untranslated region). (D) PCR products using primers as indicated in (C) were revealed by an agarose gel (1%) with SYBR Safe in the gel to stain amplified DNAs.

Europe PMC Funders Author Manuscripts

Europe PMC Funders Author Manuscripts

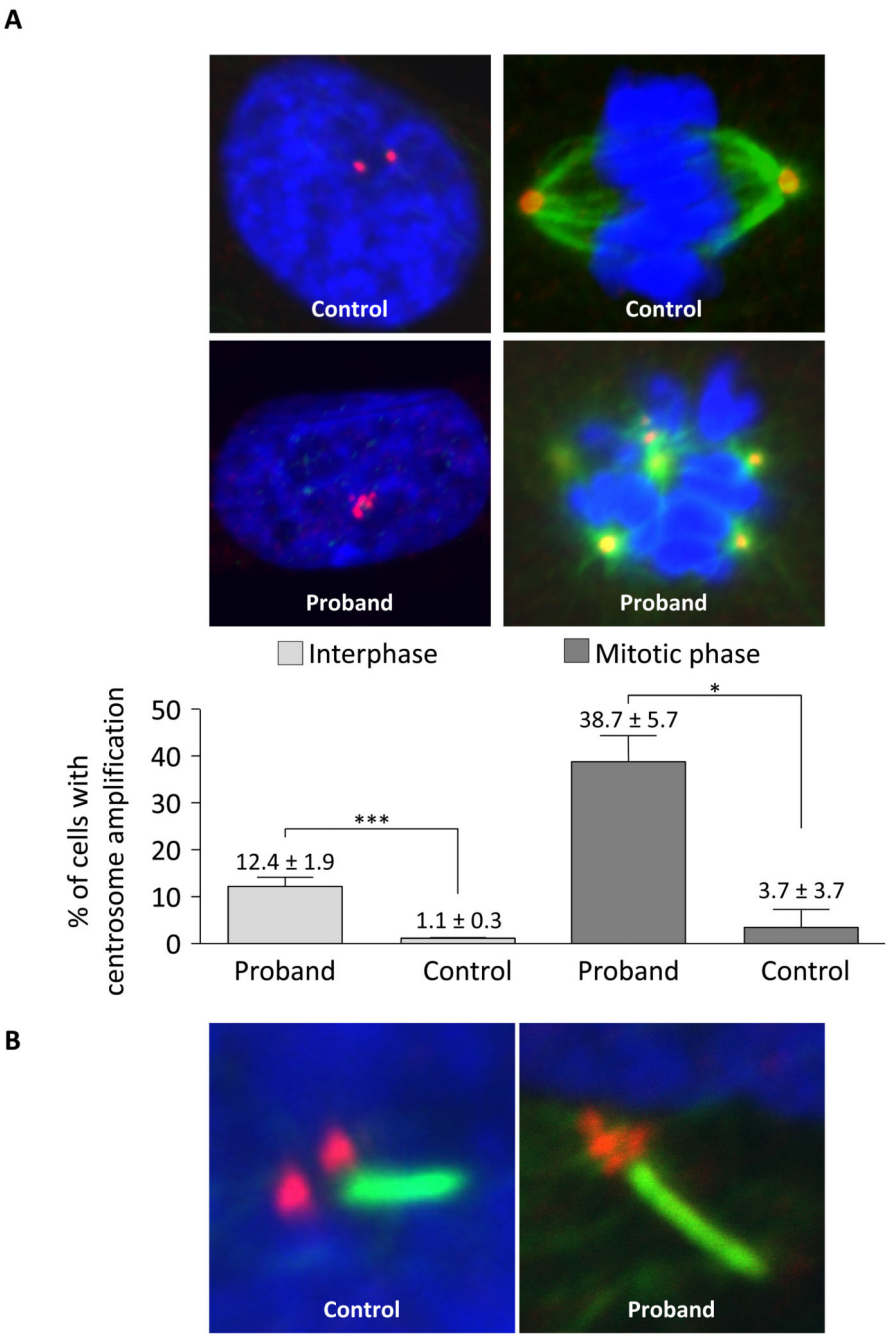

Figure 3. POC1A frameshift mutation and associated centrosome and basal body amplification

(A) Immunofluorescence analysis of dermal fibroblasts shows normal centrosome duplication and bipolar spindle formation in healthy control cells and centrosome amplification and multipolar spindle formation in proband cells. Centrosomes (red) were revealed using anti-ALMS1 antibodies and spindle fibres (green) were revealed using anti-acetylated tubulin antibodies together with appropriate Alexa Fluor conjugated secondary antibodies. Nuclei (blue) were revealed with DAPI. Bar charts show percentages of cells with centrosome amplification in interphase and mitotic phase. Error bars represent the

standard error of the mean (SEM). Asterisks indicate statistical significance (* $p < 0.05$, *** $p < 0.001$) as analysed by the Student's t test. (B) Example of amplification of the basal body (red, stained with anti-ALMS1 antibodies) of a primary cilium (green, stained with anti-acetylated tubulin) in the proband's dermal fibroblasts compared to the normal appearance of a healthy control.

Europe PMC Funders Author Manuscripts

Europe PMC Funders Author Manuscripts

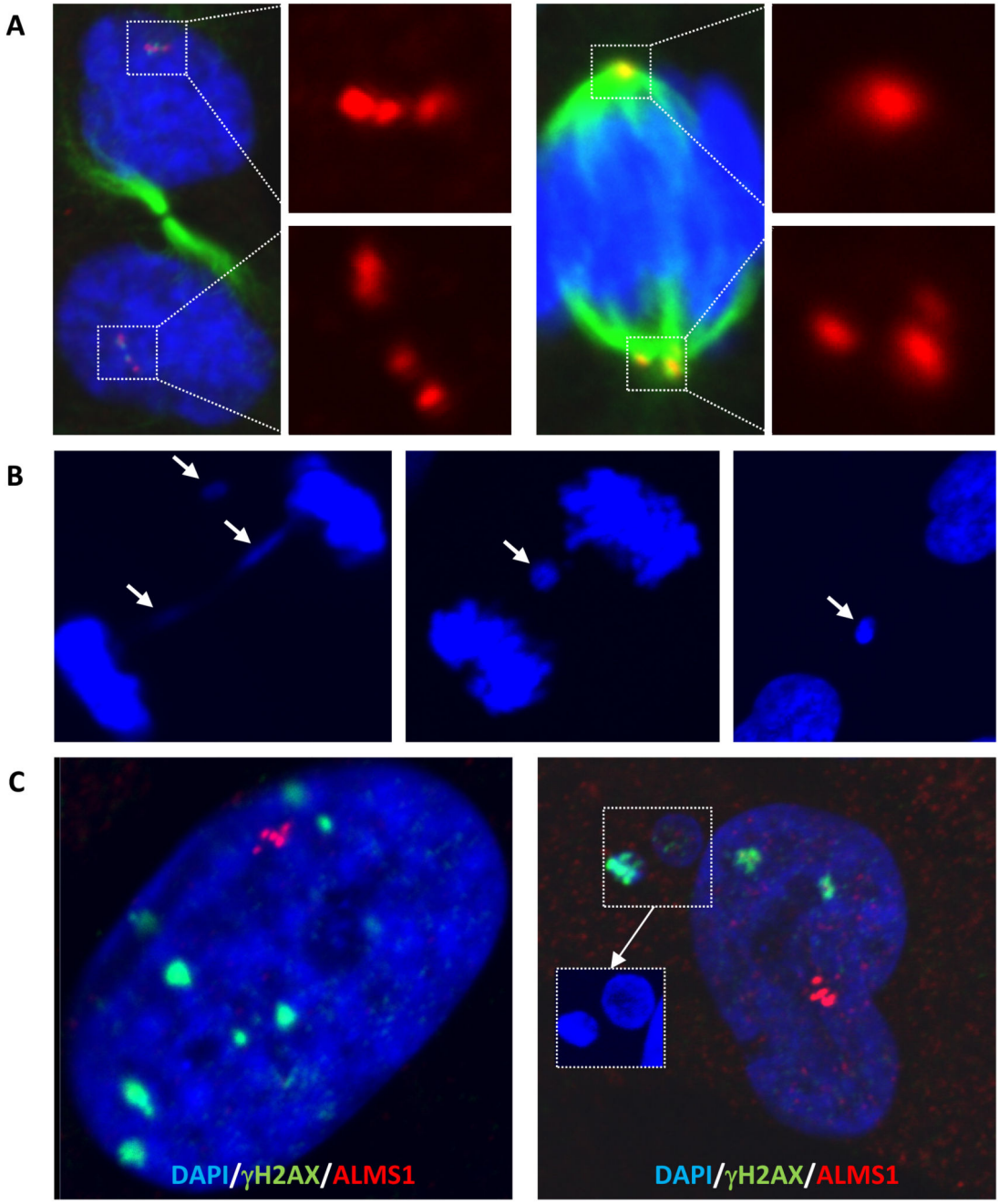

Figure 4. Centrosome clustering and evidence of DNA damage in cells harbouring centrosome amplification

(A) Centrosome clustering in proband dermal fibroblasts, with either even (left) or uneven partitioning between spindle poles (right). Immunostaining was performed using antibodies as in Figure 3. (B) Example of an anaphase bridge and resulting micronuclei formation in proband cells. (C) DNA damage foci in the nuclei and micronuclei of proband dermal fibroblasts with centrosome amplification revealed by immunofluorescence staining using anti-γH2AX antibody.

Europe PMC Funders Author Manuscripts

Table 1

Results of serial oral glucose tolerance testing of the proband

	12.7 years (no treatment)		21.3 years (no treatment)		26.4 years (metformin 1.5g/day)	
Time, mins	**Glucose, mmol/l**	**Insulin, pmol/l**	**Glucose, mmol/l**	**Insulin, pmol/l**	**Glucose, mmol/l**	**Insulin, pmol/l**
−30	--	--	5.4	201	--	--
0	4.2	532	5.1	1,675	5.0	219
10	--	--	5.2	1,661	--	--
30	6.2	4,375	9.4	5,596	7.5	1,416
60	6.2	4,494	10.2	10,290	7.1	1,978
90	5.3	5,005	11.3	12,060	8.6	3,095
120	4.6	3,514	9.1	9,985	6.9	5,108
150	--	--	8.3	10,300	--	--
180	--	--	7.3	8,089	--	--
Fasting Reference Range	<5.6	<60	<5.6	<60	<5.6	<60

Table 2
Growth and metabolic parameters of the proband at 21.3 years old

		Reference Range*
Height, m (SDS)	1.39 (−4.1)	NA
Weight, kg (SDS)	46.8 (+1.6)	NA
B.M.I., kgm^{-2} (SDS)	24.5 (+0.8)	NA
Fat, % (SDS)	34.3 (+0.8)	NA
Waist:Hip	0.84	<0.85
HbA1c, mmol/mol	31	20-38
Leptin, mg/l	32.1	2.4-24.4
Adiponectin, mg/l	0.9	2.6-12.6
SHBG, mmol/l	19.7	26-110
Testosterone, nmol/l	3.8	<2.2
Triglycerides, mmol/l	5.0	<1.7
HDL-cholesterol, mmol/l	0.69	>1.1
ALT, U/l	102	0-50
γGT, U/l	51	0-31
Liver fat, %#	108	<8

Ranges for leptin and adiponectin are BMI and sex-specific. BMI = Body Mass Index; SHBG = sex hormone-binding globulin; ALT = alanine aminotransferase; γGT = γ-glutamyl transpeptidase.

*fasting where appropriate.

#refers to the size of the magnetic resonance spectroscopy signal for triglyceride protons expressed as % of the water proto signal.